

NASA TECHNICAL NOTE



NASA TN D-5065

c.1

NASA TN D-5065



LOAN COPY: RETURN
AFWL (WLIL-2)
KIRTLAND AFB, N MEX

THEORETICAL ANALYSIS OF FLOW IN VTOL LIFT FAN INLETS WITHOUT CROSSFLOW

by Norbert O. Stockman and Seymour Lieblein

Lewis Research Center

Cleveland, Ohio



THEORETICAL ANALYSIS OF FLOW IN VTOL LIFT FAN
INLETS WITHOUT CROSSFLOW

By Norbert O. Stockman and Seymour Lieblein

Lewis Research Center
Cleveland, Ohio

NATIONAL AERONAUTICS AND SPACE ADMINISTRATION

For sale by the Clearinghouse for Federal Scientific and Technical Information
Springfield, Virginia 22151 - CFSTI price \$3.00

ABSTRACT

A method based on the Douglas incompressible potential-flow computer program has been used for the theoretical analysis of the axisymmetric flow in VTOL lift fan or engine inlets in static operation (no crossflow). The usefulness of the method for predicting flow in real inlets without flow separation was indicated by good agreement between theoretical results and limited available experimental compressible data. Example solutions were given for several different inlet configurations in which shroud curvature and depth, centerbody size and location, and inlet boundaries (type of installation) were varied. The application of the method to the design of an actual fan-in-wing inlet was given in some detail.

THEORETICAL ANALYSIS OF FLOW IN VTOL LIFT FAN INLETS WITHOUT CROSSFLOW

by Norbert O. Stockman and Seymour Lieblein

Lewis Research Center

SUMMARY

A method based on the Douglas incompressible potential flow computer program has been used for the theoretical analysis of the axisymmetric flow in VTOL lift fan or engine inlets in static operation (no crossflow). Comparison of theoretical results with limited available experimental compressible flow data indicated good agreement for the velocity distributions on the bellmouth surface and the radial velocity profiles across the passage at the end of the bellmouth. These comparisons established the usefulness of the method for predicting the flow in real inlets in which no boundary-layer separation has occurred.

Example solutions were given for several different inlet configurations in which shroud curvature and depth, centerbody size and location, and inlet boundaries (type of installation) were varied. For the range of inlet-geometry variables covered, it was found that a "trumpet" inlet was best for minimizing surface velocity gradients but that increasing depth was best for reducing radial velocity variations. Hub surface velocity gradients were small compared with those in the shroud region. Also, the flow distributions in the inlet section were negligibly affected by the type of installation, that is, wing, pod, or platform. The application of the method to the design of an actual fan-in wing inlet was given in some detail.

INTRODUCTION

In recent years, there has been much interest in vertical take-off and landing (VTOL) aircraft other than helicopters for both civil and military applications. Several different types of propulsion systems have been proposed for achieving vertical flight (see ref. 1). Among the more promising are lift fans and lift engines. For both types, since thrust for vertical lift-off is required, the propulsion system should be as light and compact as possible. Minimum engine volume is also desired to minimize drag if the lift propulsion system is carried along in pods during normal cruise flight.

One of the factors involved in achieving minimum weight and volume for a lift fan or lift engine is the design of an efficient shallow inlet. In the case of a lift fan installed in a wing, the inlet depth may be restricted to small values by the available maximum thickness of the wing section.

A shallow fan or engine inlet, however, presents two major aerodynamic problems: (1) unfavorable velocity gradients on the bellmouth surface may lead to excessive boundary-layer growth and separation, and (2) large radial variations in velocity across the passage may make the design of the fan or compressor more difficult or the operation less efficient. Such effects may appear when a VTOL aircraft is operating in the landing, takeoff, or hover mode for which the inlet is essentially operating statically with no significant free-stream velocity relative to the airplane, as well as when the inlet is operating in a cross flow (aircraft in the transition mode). The satisfactory solution to these problems will depend on reasonably accurate methods for estimating the surface velocity distributions and passage velocity profiles induced by various inlet configurations. In addition, these methods can be used to provide information on the radial variation of the flow at the inlet of the fan or compressor rotor. Such input data are necessary for the proper design of the blading of the fan or compressor. A first step in the pursuit of such methods is an analysis of the flow in inlets under static conditions.

Some studies have been made and published of the flow in VTOL inlets in static operation. These studies consist of both plane two-dimensional theoretical analyses (e. g. , refs. 2 to 5) and experimental studies (e. g. , refs. 2, 4, and 6 to 10). However, the theoretical methods reported in the references are based on plane two-dimensional incompressible potential flow in inlets without centerbodies. A real VTOL inlet will be axisymmetric or three-dimensional, and, in the case of a lift fan, will have a centerbody in the bellmouth resulting in an annular passage.

A comprehensive method of calculating the incompressible potential flow for a complete fan-in-wing configuration, including the wing, the inlet, and the fan efflux is reported in reference 11. This method can produce the velocity and pressure at any point on the surface or in the airstream in the inlet for a prescribed distribution of fan inflow velocity and a prescribed free-stream velocity. However, it may not be practical to use the method of reference 11 for solutions of the flow in just the inlet section in static operation because of the lengthy input setup time and computer running time.

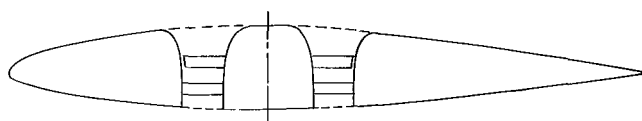
An incompressible potential-flow computer program (the Douglas potential flow program) for finding the flow through axisymmetric inlets has been developed by Smith, et al. (refs. 12 to 14). This program was not specifically applied to VTOL inlets; however, theoretical calculations of pressure distributions were made for a propeller shroud in static operation, and the results were found to agree quite well with experimental results.

This report presents an analysis of flow into VTOL inlets in static operation based

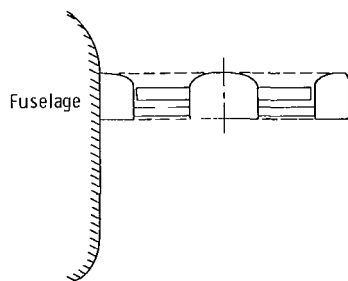
on the Douglas potential flow program. Included in the study are several comparisons with available experimental results and a comparison with a two-dimensional solution. Parametric solutions of inlets are then investigated in which bellmouth curvature, axial depth, centerbody size and location, and type of installation are varied. Finally, application of the method to fan-in-wing inlet design is treated.

ANALYSIS

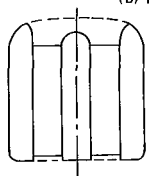
Examples of inlet configurations that might be used in VTOL lift fan or lift engine installations are shown in figure 1. The inlet configurations are all similar in principle, with minor differences resulting from type of power unit and installation. Results of the gross effects of geometry changes on flow variations in any particular type of VTOL installation should be generally applicable to the others. In this report, attention will be focused primarily on the fan-in-wing installation as the reference system.



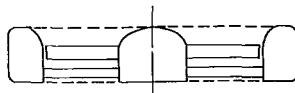
(a) Lift fan in wing.



(b) Lift fan in fold-out platform.



(c) Lift engine in wing pod or fuselage.



(d) Lift fan in wing pod.

Figure 1. - Inlet configurations for various VTOL installations.

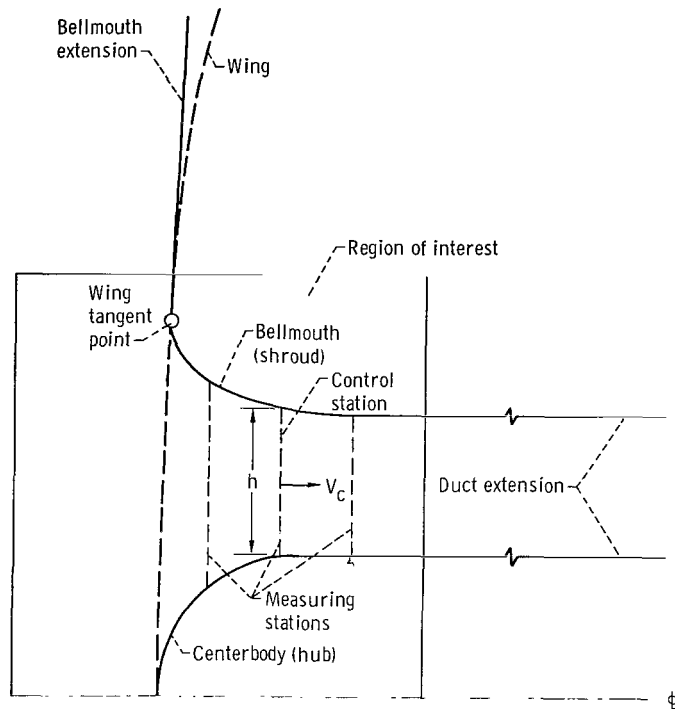


Figure 2. - Meridional profile of idealized fan-in-wing inlet for potential-flow solution. Annular passage height, h ; control-station velocity, V_c .

The idealization of the VTOL inlet for use in the potential-flow analysis is shown in figure 2. This differs from the real inlet in that (1) a duct extending far downstream is added to the inlet at the downstream end of the region of interest (region in which solution values are desired), (2) the wing or upper surface is simulated by a cone (in the limit a flat plate) tangent to the bellmouth and extending far into the free stream, and (3) the ideal inlet is axisymmetric over the entire length, whereas, the real one may not be in the upper bellmouth region, depending on the particular installation. A way of handling asymmetric inlets will be discussed later.

Frequently, there will be one or more stations of interest located at a definite axial depth in the inlet. Such locations, called measuring stations (fig. 2), represent stations for which test data are available or for which flow properties are desired, such as a rotor inlet. In addition, the solution procedure requires that the average axial velocity be specified at one of the measuring stations called the control station. The location of the control station is arbitrary, although it is generally taken at the inlet plane of the engine or fan.

The problem, then, is to determine the potential flow solution corresponding to the prescribed average axial velocity at the control station. A solution consists of velocity distributions along the hub and shroud surfaces and velocity profiles at the measuring

stations. A solution may also include velocities in the flow field, that is, the velocity vectors at specified points above the wing or inlet.

Assumptions and Equations

The geometric configuration of the inlet section is assumed to be axisymmetric with meridional contours of arbitrary shape. For this geometry, the flow is assumed to be axisymmetric, incompressible, and inviscid. The basic conditions of incompressible, inviscid flow are conservation of mass and irrotationality. These two conditions lead to the Laplace equation

$$\nabla^2 \Phi = 0 \quad (1)$$

where Φ is the velocity potential and is related to the local velocity vector \bar{V} by

$$\bar{V} = \nabla \Phi \quad (2)$$

The boundary condition of zero normal velocity at a surface is

$$(\nabla \Phi) \cdot \bar{n} = \frac{\partial \Phi}{\partial n} = 0 \quad (3)$$

where \bar{n} is the outward-pointing vector normal to the surface. Furthermore, to ensure uniqueness of the solution, the regularity condition at infinity is specified as

$$|\nabla \Phi| \rightarrow 0 \quad (4)$$

Equations (1), (3), and (4) comprise the problem to be solved.

A computer program for the solution of the potential flow problem for axisymmetric shapes developed by Smith, et al., is reported in references 12 and 13. In reference 14 a method is presented for applying the potential flow program of references 12 and 13 specifically to the calculation of flow about inlets. The method of reference 14 has been used in the present study to determine the potential flow in VTOL inlets in static operation corresponding to a prescribed average axial velocity at the control station.

Inlet Surface Coordinates

The Douglas potential-flow program requires that the inlet geometry be input in the form of a separate set of discrete coordinate points for each body. An annular inlet (fig. 2) consists of two separate bodies: the centerbody (or hub), including its extension, and the bellmouth (or shroud), including its extensions. To facilitate the accurate and rapid generation of coordinate points that determine the surfaces of the bodies, a computer program was developed at the Lewis Research Center utilizing a limited combination of straight lines and superellipses. A superellipse (ref. 15) is a curve of the form

$$\left(\frac{x}{a}\right)^n + \left(\frac{y}{b}\right)^n = 1 \quad (5)$$

where n may take on any real value greater than 1.0. When $n = 2$, the curve becomes an ellipse (or circle if $a = b$). Only one quadrant of the superellipse is used, and straight lines are fitted at the ends. Thus, between two fixed straight lines, a wide variety of curvature distributions can be obtained by varying the exponent n . Another advantage of the superellipse is that the end points (of one quadrant of the curve) have

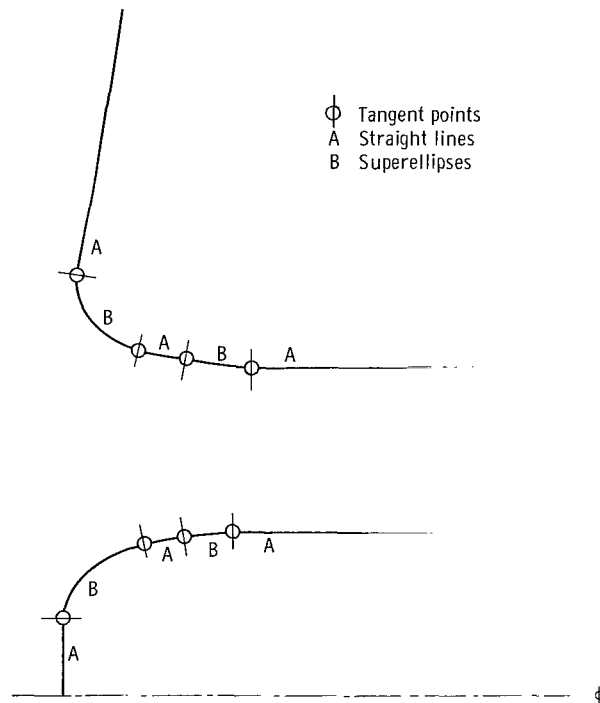


Figure 3. - Inlet constructed of superellipses and straight lines.

zero curvature when $n > 2$, and can thus be fitted to straight lines without a discontinuity in curvature.

The superellipse program is set up in such a way that both the centerbody and the bellmouth may be represented by a contour made up of at most two superellipses separated by straight lines and enclosed by straight lines (fig. 3).

Applicability

Inasmuch as a real inlet involves compressible flow with surface boundary layers, and, in some cases, bellmouth contours that are not exactly axisymmetric (e. g., inlet for fan in wing), some prior discussion of the applicability of the solution method for real inlets is in order.

Potential flow solutions are known to provide an adequate representation of the flow around bodies if the surface boundary layers are unseparated, and thin compared with the flow passage height and if there are no large areas with total-pressure gradients in the free-stream flow outside the boundary-layer regions. VTOL inlets are generally open and relatively free of external components, so that the condition of a clean, free-stream flow will generally be met. Furthermore, it is presumed that a final design configuration will be one in which boundary-layer separation is prevented. Thus, the potential flow model should be a valid representation of the real flow for design purposes. It should also be valid for the calculation of the flow in a given inlet as long as the boundary layers are unseparated.

Theoretically, when boundary layers are present on curved surfaces, such as in the case of the inlet bellmouth, the variation in static pressure across the boundary layer may not be precisely the same as that calculated by the potential flow model. Thus, predicted surface pressures may be somewhat in error. However, such differences are expected to be very small for thin layers. Furthermore, this effect should be negligible in comparison with the other discrepancies between the real flow and model flow as discussed herein.

In the application of the method, the input control-station axial velocity should be prescribed for the real case according to compressible flow considerations. Thus, any effect of compressibility in the solution will depend on the difference between the Mach numbers at the local points of interest and the Mach number at the control station. The control station in most cases will be located at the inlet to the fan or engine compressor. Lift fans and engine compressors are generally designed for relatively high subsonic inlet Mach numbers (of the order of 0.6), so that the differences between these values and the critical velocity values (i. e., peak surface velocities) will not generally be large. Errors due to compressibility effects might be largest for the low velocities, which will

generally not be of concern. Thus, it is expected that the absence of compressibility considerations in the method will not be a serious limitation in the usefulness of the solution for real compressible flows.

When an asymmetry of the inlet is present, as in the case of a fan-in-wing inlet (i. e., fore and aft bellmouth contours are different than the spanwise contours), it is expected that the axisymmetric solution can still be used to provide accurate results. For such a case, an axisymmetric solution can be obtained for each contour at the major circumferential locations involved. The solution for each contour is considered to be applicable only at the location of that contour. Thus, a discrete variation in velocity profiles around the periphery of the inlet is obtained. The correspondence between the velocities so obtained and a true asymmetric solution will depend on the magnitude of the circumferential gradients of the bellmouth contour compared with the gradients of curvature in the axial direction. For fan-in-wing installations, this relative rate of change of contour curvature with circumferential distance will not be large. Thus, the succession of solutions should provide a close approximation to the true circumferential variation of flow in moderately asymmetric inlets.

COMPARISONS

In order to further explore the applicability of the method of calculation in predicting the real compressible flow field in VTOL inlets, theoretical results will be compared with available experimental data. Also, in order to give some idea of the usefulness of plane two-dimensional potential-flow solutions in representing an axisymmetric flow, a comparison will be made between an axisymmetric and a two-dimensional potential-flow solution.

Very little detailed information is available for actual velocity distributions on inlets in static operation. However, two cases of published data and two cases of unpublished data have been obtained for comparison with theory. These consist of one configuration with radial-velocity profiles, which will be presented first, and three configurations with surface-pressure distributions, which will be presented in order of increasing Mach number. In an attempt to better approximate the real compressible flow, the theoretical calculations were based on a compressible average axial velocity at the control station. Surface pressures, where required, were obtained from the theoretical surface velocities by means of compressible-flow relations. For all the cases considered, there was no indication of boundary-flow separation on the bellmouth or centerbody surfaces.

Passage Velocity Profile Data

In reference 9, some test results are given for a small suction model of a fan inlet. The configuration obtained from figure 6 of reference 9 is shown in the inset of figure 4. Also shown are the experimental velocity profiles at three velocity levels taken in a measuring plane representing the approximate location of the rotor inlet. The precise axial location of the measuring plane is not available, but it is around 1/4 to 3/8 inch (0.635 to 0.952 cm) downstream of the plane where the circular arcs of the bellmouth and centerbody become tangent to the walls of the duct. For this reason theoretical velocity profiles were obtained at stations 1/4 and 3/8 inch (0.635 and 0.952 cm) downstream of the tangent points and are shown in figure 4. The average velocities at the control station for the potential flow were taken to be the integrated area average of the

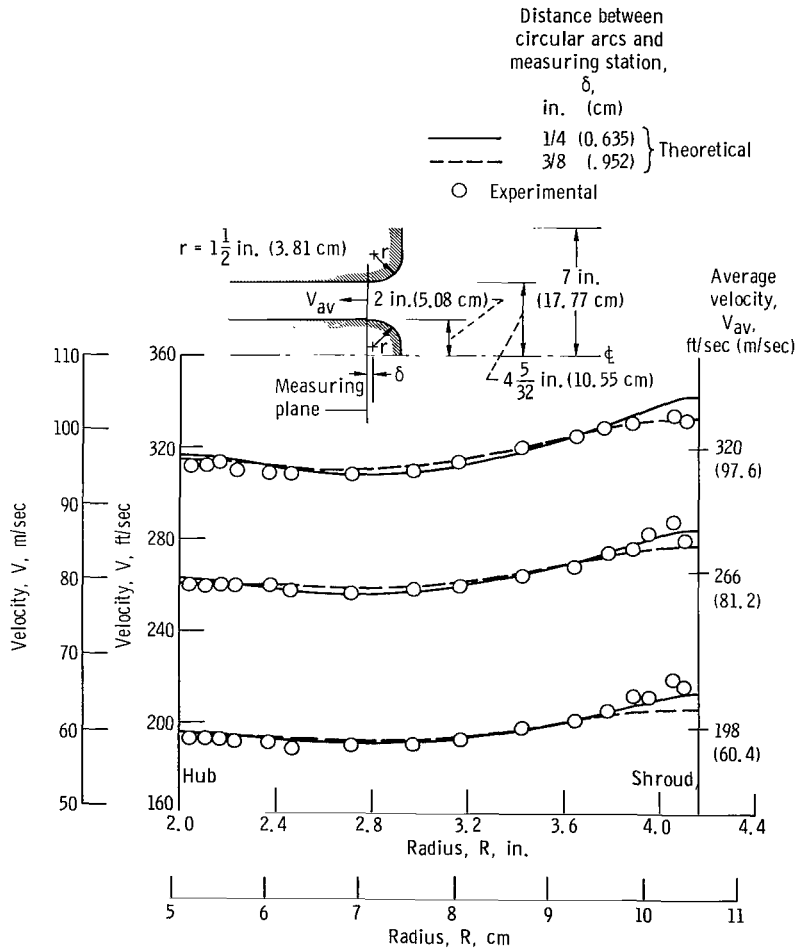


Figure 4. - Velocity profiles at rotor inlet station of annular bellmouth. Comparison of potential-flow theory with experimental results. (Data from ref. 9.)

experimental velocity profiles. The agreement is seen to be quite good except near the shroud where an unstable flow region was noted in the experiments.

Surface Velocity Data

Low Mach number. - In references 2, 6, and 7, tests of several suction-model fan-in-wing inlet configurations are reported. The main emphasis in these publications is on cross flow conditions, and only limited static test results are included. However, additional surface pressures were made available by the authors. Data for the datum configuration of references 6 and 7 under nearly static conditions and at relatively low-flow Mach numbers were accordingly obtained from the National Research Council of Canada. The test inlet was set in a two-dimensional wing and was therefore not axisymmetric. The forward inlet profile in a chordwise section is shown in the insert in figure 5. The axisymmetric configuration for the theoretical solution was generated by revolving this profile about the centerline. The operating test conditions were an average velocity V_c over the active flow area at the measuring station ($S = 0$ in fig. 5) of 214.04 feet per sec-

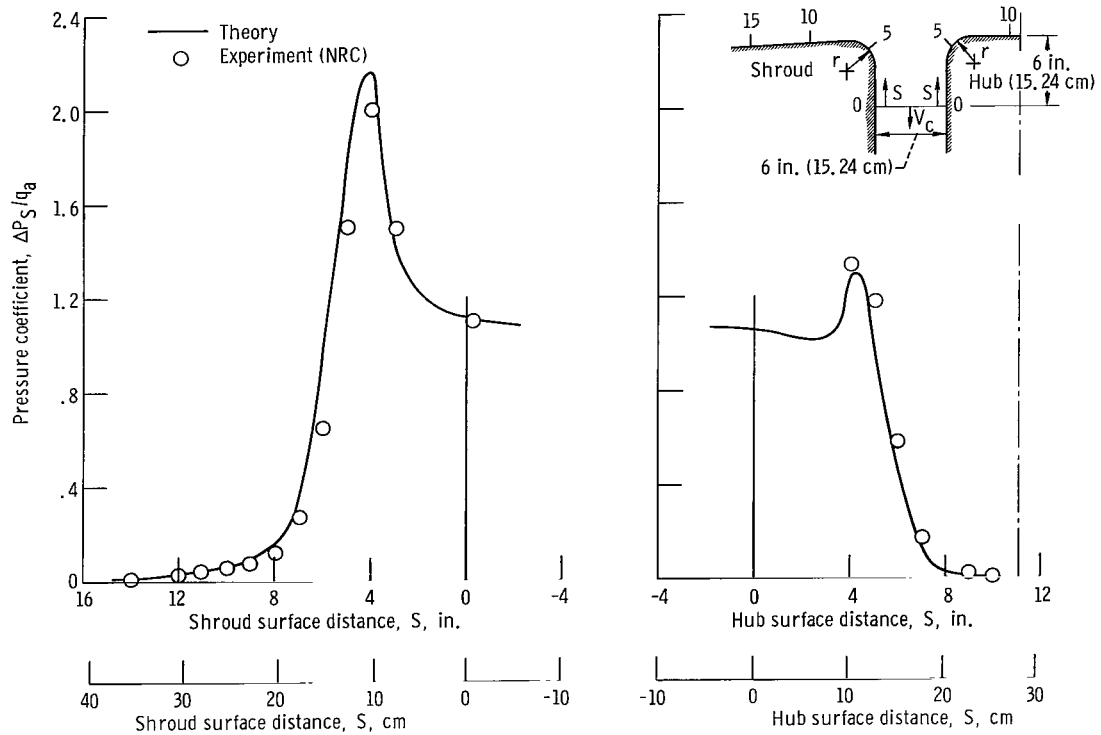


Figure 5. - Surface-pressure distribution on forward portion of 24-inch (60.96-cm) diameter fan-in-wing inlet; comparison of theory with experiment (data from NRC of Canada). Control-station velocity, V_c , 214 feet per second (65.2 m/sec); radius of curvature, r , 2.16 inches (5.48 cm).

ond (65.2 m/sec) and a slight cross flow, possibly from both the fore and aft directions, since the tests were conducted in a wind tunnel open at both ends. In matching theory with experimental results, the average velocity at the control station is taken to be equal to the average experimental velocity over the active-flow area; that is, the area occupied by the boundary layer is excluded from the area-averaged velocity.

The experimental and theoretical results were expressed in terms of the parameter $\Delta P_s/q_a$, which is the difference between the ambient total pressure and local static pressure divided by the bulk-velocity dynamic pressure. This parameter is obtained from

$$\frac{\Delta P_s}{q_a} = \frac{P_t}{\frac{1}{2} \rho_a V_a^2} \left(1 - \frac{P_s}{P_t} \right) \quad (6)$$

where P_t is the standard ambient total pressure, ρ_a is obtained from V_a and standard conditions, and V_a is the bulk velocity, that is, the average velocity over the geometric area, and is equal to 205.76 feet per second (62.6 m/sec). The pressure ratio P_s/P_t is obtained from the theoretical velocity V and the compressible flow relation

$$\frac{P_s}{P_t} = \left[1.0 - 0.2 \left(\frac{V}{a_t} \right)^2 \right]^{3.5} \quad (7)$$

where a_t is the stagnation speed of sound obtained from

$$a_t = \sqrt{1.4 RT_t}$$

where the gas constant R is equal to 1715.6 square feet per second squared per $^{\circ}R$ ($287 \text{ m}^2/(\text{sec}^2)(K)$) and T_t the total temperature, is prescribed.

It can be seen in figure 5 that the theory agrees quite well with the experiment. On both hub and shroud, the trend of the theoretical pressure distribution is quite similar to the experimental and the location of the theoretical peak seems to be close to the experimental.

Medium Mach number. - In reference 8 results are given of static tests of a 12-inch (30.48-cm) diameter fan submerged in a wing, including one example of a surface-pressure distribution on the forward hub and shroud surfaces of the inlet. This pressure distribution was obtained at a fan rotor speed of 15 000 rpm and a bulk inlet Mach number of 0.53 at the measuring station (fig. 6). The data taken from figure 11 of

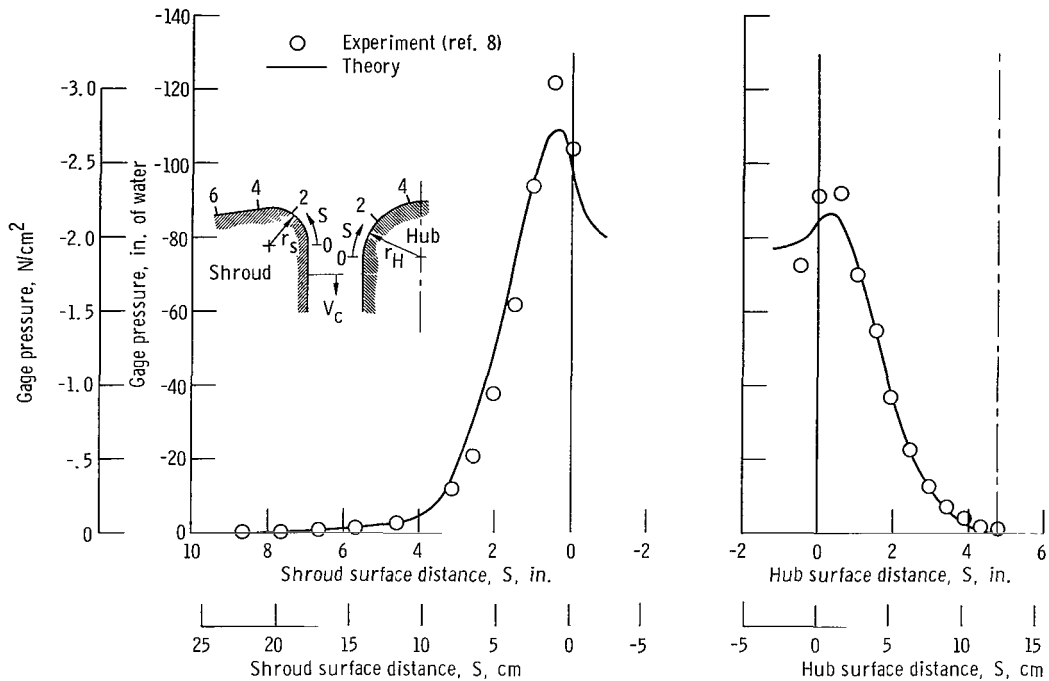


Figure 6. - Surface-pressure distribution on forward portion of 12-inch-diameter fan-in-wing inlet; comparison of theory with experimental data of reference 8. Control-station velocity, V_c , 604 feet per second (184 m/sec); shroud radius of curvature, r_s , 2.0 inches (5.08 cm); hub radius of curvature, r_H , 3.0 inches (7.62 cm).

reference 8 expressed in terms of gage pressure, $P_t - P_s$, are shown in figure 6. Also shown is the forward portion of the chordwise profile of the inlet. This profile was used as the axisymmetric configuration for the potential flow solution. The bulk inlet velocity at the measuring station obtained from the Canadian National Research Council was 575 feet per second. If this velocity is increased by 5 percent to account for boundary-layer blockage, then the average active-flow-area velocity V_c is 604 feet per second (184 m/sec). This velocity was used to obtain the theoretical results which are shown in figure 6. The agreement is satisfactory for engineering use but not quite as good as in figure 5. However, the exact value of the average active-area velocity (or, equivalently, the effective boundary-layer blockage) is not known, so that a more precise comparison cannot be made. Still, the theory gives a quite useful prediction for the trend of the curve and the location of the peak velocity.

High Mach number. - Some unpublished data taken on a suction model of a fan-in-wing inlet were obtained from the General Electric Co., Cincinnati, Ohio. The test inlet model for which the data were obtained is reported in reference 16. The test model was a 10-inch (25.4-cm) diameter inlet with a circular-arc bellmouth (arc-radius-to-inlet-

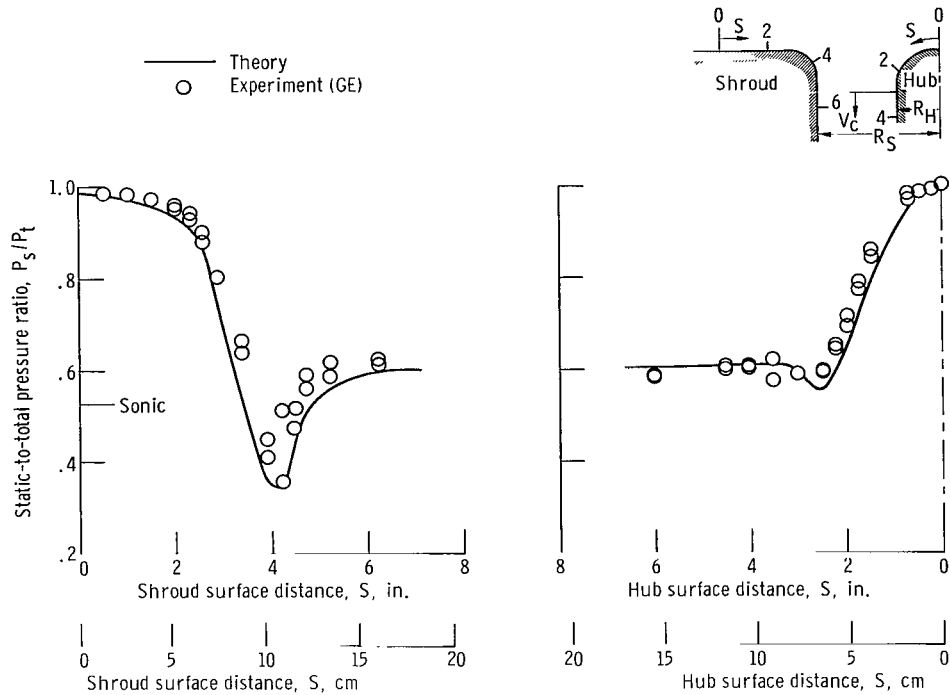


Figure 7. - Surface pressure distribution on 10-inch (25.4-cm) diameter suction model inlet. Comparison of theory with experiment (data from G. E.). Control-station velocity, V_C , 928 feet per second (283 m/sec); hub radius, R_H , 1.79 inch (4.55 cm); shroud radius, R_S , 5.1 inch (12.96 cm).

diameter ratio of 0.12) as shown in figure 7. The data obtained consist of surface-pressure distributions taken at a high velocity as shown in figure 7. In spite of the existence of local supersonic velocities on the bellmouth, there was no indication of flow separation; therefore, this case should be amenable to the potential flow method of solution. However, because of the very high average Mach number (around 0.9) it does present a rather severe test of the applicability of the method. Furthermore, the average velocity across the inlet at some measuring station was not accurately known and was estimated from the downstream hub and shroud surface pressure ratio to be 928 feet per second (283 m/sec) at the control station (fig. 7). The resulting theoretical pressure distribution is shown in figure 7. One further fact should be pointed out, namely, that there was some unresolved discrepancy between the surface distance measurement of the test model and that of the theoretical configuration. Since previous results indicate that the theory accurately predicts the location of the velocity peak, the surface distance scales were lined up to coincide at this point. Once again, as indicated in figure 7, the theory predicts the trend quite well and is reasonably close to the experimental values even in the region of local supersonic velocities.

Plane Two-Dimensional Solution

Often a plane two-dimensional potential-flow method of solution may be available when an axisymmetric one is not, or existing plane two-dimensional results may be available (e.g., refs. 2 to 4) that can be applied to axisymmetric configurations. It is of interest, therefore, to have some appraisal of the differences between the two solutions and the areas where comparable solutions might be obtained.

The difference between the plane two-dimensional and axisymmetric formulations of potential flow originates in the continuity equation which is equivalent to the Laplace equation (eq. (1)) written in terms of velocity components instead of the potential function. In an $R - Z$ plane, the plane two-dimensional continuity equation is

$$\frac{\partial V_Z}{\partial Z} + \frac{\partial V_R}{\partial R} = 0 \quad (8)$$

and the axisymmetric formulation is

$$\frac{\partial V_Z}{\partial Z} + \frac{\partial V_R}{\partial R} + \frac{V_R}{R} = 0 \quad (9)$$

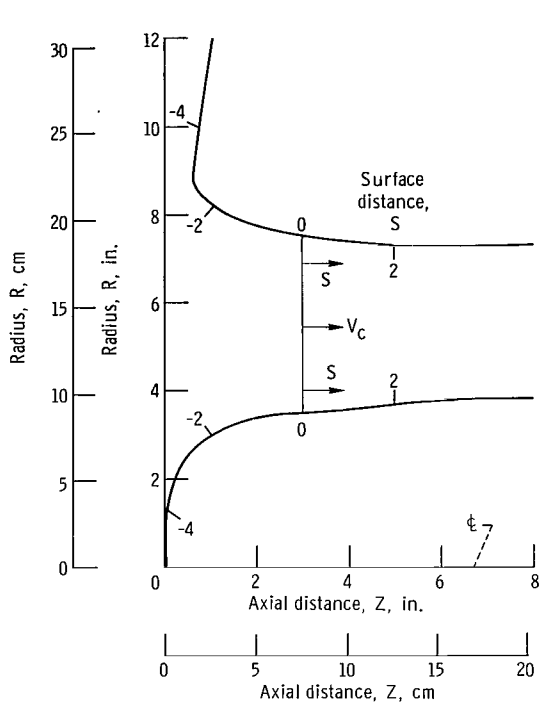
where V_Z and V_R are the axial and radial velocity components, respectively. The difference between these two equations is the term V_R/R . In order to evaluate the importance of this term in affecting the solution differences, it is necessary to recast equations (8) and (9) in the form

$$\frac{\partial V_Z / \partial Z}{\partial V_R / \partial R} = -1.0 \quad (10)$$

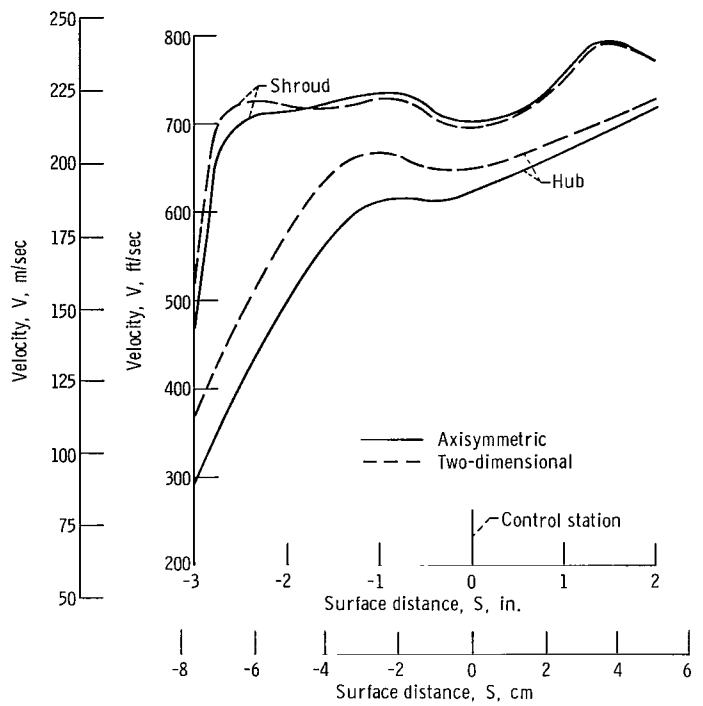
and

$$\frac{\partial V_Z / \partial Z}{\partial V_R / \partial R} = - \left(1.0 + \frac{V_R / R}{\partial V_R / \partial R} \right) \quad (11)$$

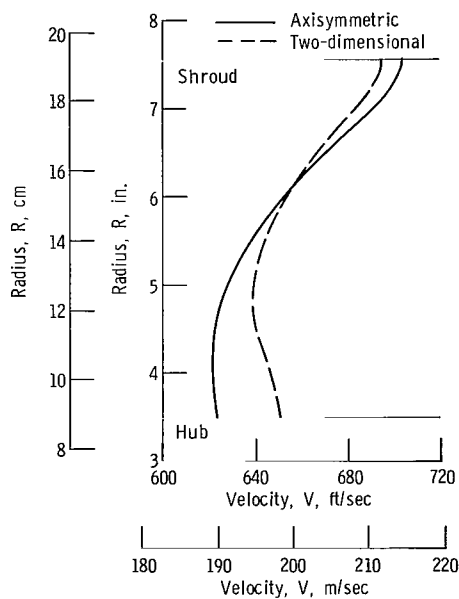
Thus, it appears that good agreement could be expected between the two cases in regions where $(V_R/R)/(\partial V_R/\partial R)$ is small compared with 1.0. The degree of agreement, however, will be affected by the extent of the region of small $(V_R/R)/(\partial V_R/\partial R)$ and the relative influence of the region of larger $(V_R/R)/(\partial V_R/\partial R)$, since regions of larger $(V_R/R)/(\partial V_R/\partial R)$ have the effect of producing boundary conditions on the region of small $(V_R/R)/(\partial V_R/\partial R)$ that differ between the two-dimensional and axisymmetric cases.



(a) Inlet geometry.



(b) Surface velocity distribution.



(c) Passage velocity profile at control station (surface distance, 0).

Figure 8. - Comparison of two-dimensional with axisymmetric potential flow solutions. Control-station velocity, V_c , 650 feet per second (198 m/sec).

Thus, a general quantitative criterion for the agreement in local regions of the flow field cannot be given.

In order to give a more concrete indication of the usefulness of plane two-dimensional solutions, the two types of solutions will be compared for one inlet configuration. The two-dimensional solution was obtained from the Douglas plane potential-flow program (refs. 12 and 13) in the same manner as described herein for the axisymmetric program. The inlet geometry selected for the comparison calculation is shown in figure 8(a).

The resulting hub and shroud surface velocities are compared with the axisymmetric program results on figure 8(b). The agreement on the shroud is very close (except in the region of greatest curvature where V_R is greatest), but the agreement on the hub is not nearly as good because of the smaller value of R . The velocity profiles across the passage for the same inlet are compared in figure 8(c). These profiles are located at the control station of this particular inlet ($S = 0$ in fig. 8(a)). The agreement near the tip or shroud is probably adequate; however, the agreement near the hub is poor, and the accuracy may be inadequate for rotor blade design. The agreement of radial profiles upstream of the reference station will be worse, as can be inferred from the hub-surface velocity comparison on figure 8(b).

In summary, a plane two-dimensional solution will probably be adequate for investigating the shroud-surface-velocity variation (e.g., for avoidance of peaks or for boundary-layer calculations), but may not be adequate in predicting velocity profiles across the passage.

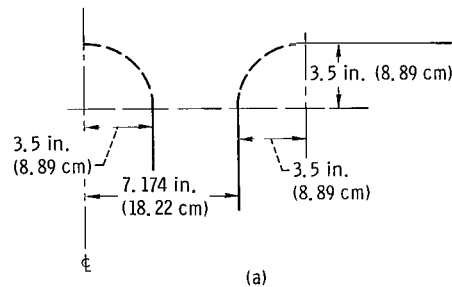
EXAMPLE SOLUTIONS

In this section the effect of geometric configuration variables such as bellmouth curvature, centerbody location (axial depth), and ratio of the hub radius to the shroud radius (hub-tip ratio) at the control station on the velocity distributions will be presented. Also shown will be the effect of axial depth on the radial velocity profile for given configurations. Finally, the effect of varying the external boundaries of the inlet resulting from different installations will be indicated.

Most of the example solutions will be presented in dimensional form. However, inspection of equations (1) to (4) indicates that any solution will, in general, also hold for all scaled geometries and velocities. Thus, the solutions given herein can readily be made dimensionless by dividing the lengths by a reference length (such as the inlet outer radius or the passage height) and by dividing the velocities by the prescribed control-station velocity. Dimensionless values can, in turn, be converted to other dimensional quantities by multiplying by the appropriate normalizing factors.

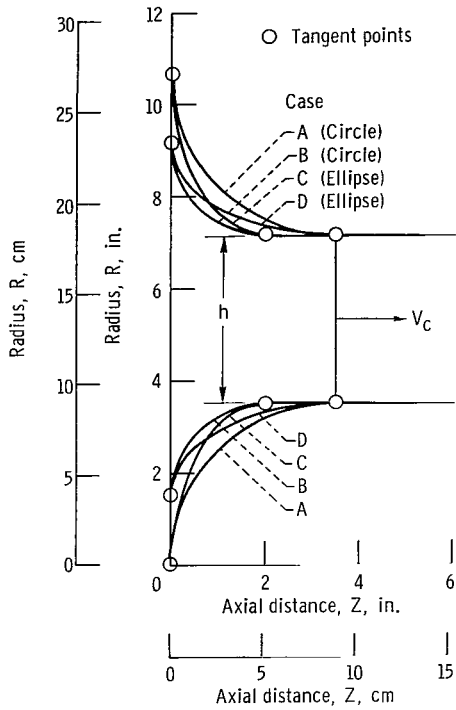
Effect of Curvature Distribution

The flow passing along the bellmouth surface and into the inlet must turn through approximately 90° for a VTOL inlet. This turning requires a certain amount of curvature of the bellmouth surface. The velocity distribution along the surface is very sensitive to the manner in which the curvature is distributed along the surface. The radial variation of velocity at some axial station of interest in the inlet (e.g., the rotor inlet station of a lift fan) is also sensitive to the curvature distribution. To illustrate these sensitivities and to indicate what type of curvature distributions might be desirable, several simple curvature distributions were investigated. The basic configuration examined is an inlet with a flat upper surface, a straight section shroud radius of 7.174 inches (18.22 cm), a hub-tip ratio of 0.488, and maximum allowable depth and width of 3.5 inches (8.89 cm) each for curvature distribution (see sketch a).

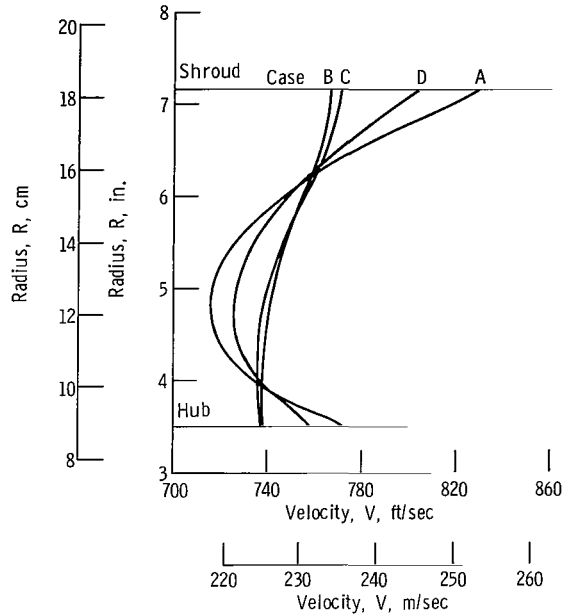


Circles and ellipses. - The first four curves to be considered are shown on figure 9(a). These are circular arcs with a radius of 3.5 inches (8.89 cm) (case A) and 2.0 inches (5.08 cm) (case B), and ellipses with the major axis equal to 3.5 inches (8.89 cm) and the minor axis equal to 2.0 inches (5.08 cm) in two orientations (cases C and D), as shown in figure 9(a). Where necessary, the curves are fitted to straight lines to fill out the basic configurations. The points of tangency of the curves to the straight lines are also indicated on the figure.

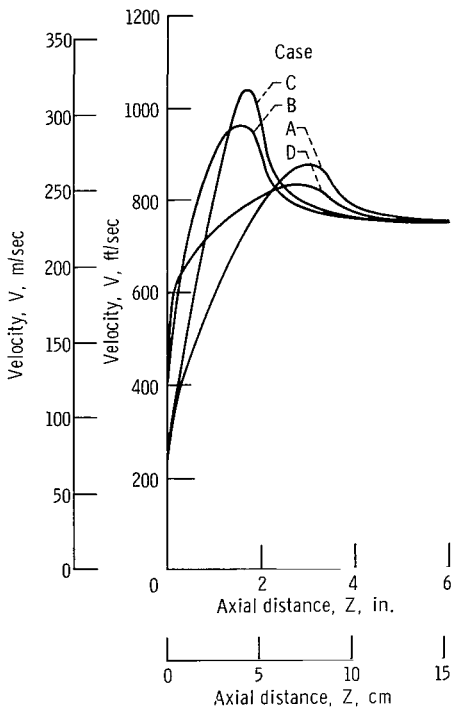
The velocity profiles at an inlet depth of 3.5 inches (8.89 cm), which represents a ratio of depth to passage height approximately equal to 1.0, are shown on figure 9(b). Cases A and D, whose curvature persists to the 3.5-inch (8.89-cm) station have more severe radial gradients than cases B and C whose curvature stops at a depth of 2.0 inches (5.08 cm). Thus, it appears that the chief variable affecting the straightness of the velocity profile is the depth of the curving section rather than the distribution of curvature. As might be expected, the greater the length of the straight section between the curved section and the measuring plane, the less severe the velocity variation at the



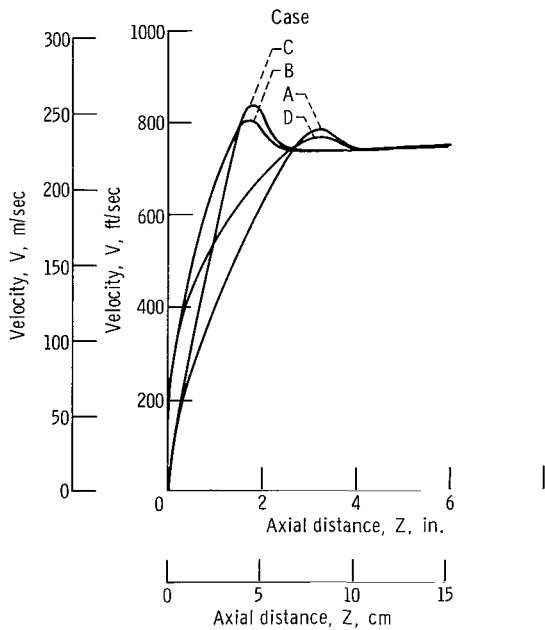
(a) Inlet geometry.



(b) Passage velocity profile. Control station depth, 3.5 inches (9.89 cm); control station depth to passage height ratio, 0.952.



(c) Shroud-surface-velocity distribution.



(b) Hub-surface-velocity distribution.

Figure 9. - Effect of inlet curvature distribution on potential-flow solution. Control-station velocity, V_C , 750 feet per second (229 m/sec).

measuring plane. However, for a given depth of curved section, the ellipse with major axis parallel to the inlet centerline (case D) has a somewhat better passage profile than the circle (case A) because the ellipse has less curvature near the measuring station.

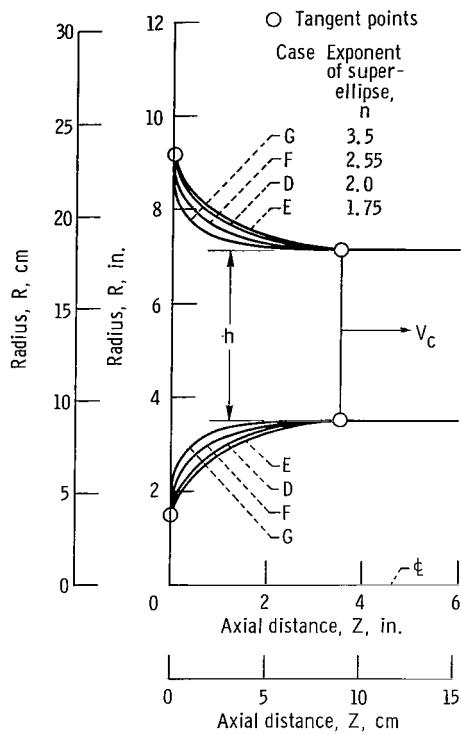
The shroud-surface-velocity distributions are shown on figure 9(c). In all cases, the velocity peak is located a short distance upstream of the point of transition from curved to straight section (tangent point in fig. 9(a)). The magnitude of the peak velocity is less when the curvature is distributed over a greater depth (cases A and D). For a given depth of curved section, the ellipse with major axis parallel to the centerline (case D) has a more favorable surface-velocity distribution than the circle of case A, but the circle (case B) is better in this respect than the ellipse with major axis perpendicular to the fan centerline (case C).

The hub-surface-velocity distributions are shown on figure 9(d). Since the hub contours are composed of the same curves as the corresponding shroud contours (see fig. 9(a)), the velocity distributions are similar to those on the shroud. However, the level of peak velocity in the bellmouth region is lower on the hub because less flow is drawn in along the hub. In considering the overall desirability of the various cases, a compromise is indicated because cases A and D have better surface-velocity distributions, whereas cases B and C have more uniform passage-velocity profiles at the station $Z = 3.5$ inches (8.89 cm).

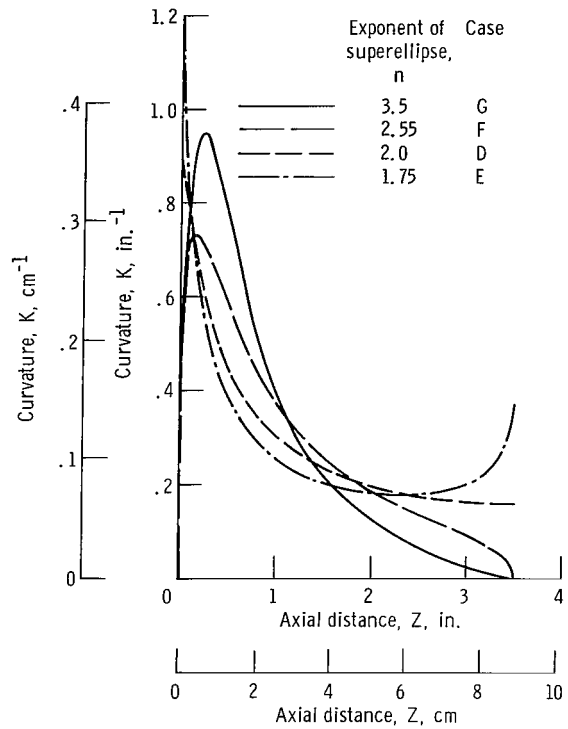
Superellipses. - Since case D has the best surface-velocity distribution, it was chosen to be the basic configuration for studying the effect of the superellipse exponent n of equation (5). In addition to case D ($n = 2.0$), three more cases, E, F, and G were considered having n 's of 1.75, 2.5, and 3.5, respectively. The configurations are shown in figure 10(a). These are all similar to the trumpet inlet configuration recommended in reference 3. The curvature distributions of the four cases are shown on figure 10(b).

The passage velocity profiles at a depth of 3.5 inches (8.89 cm) are shown in figure 10(c). It can be seen that the greater the value of n , the less severe the radial velocity variation. This is because, as n is increased, the curvature becomes less near the measuring station at 3.5 inches (8.89 cm) (see fig. 10(b)).

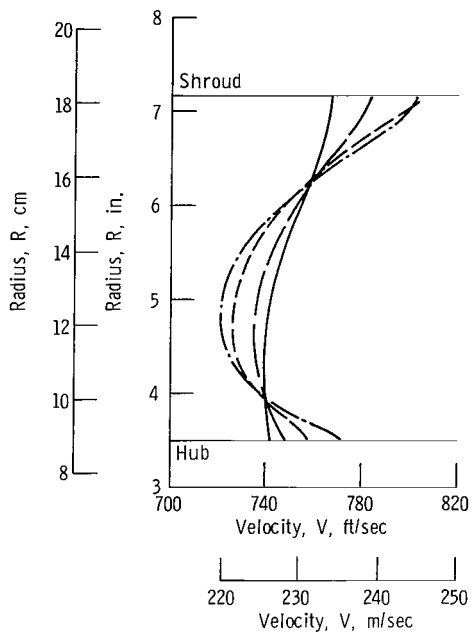
The shroud-surface-velocity distributions are shown on figure 10(d). (The hub-velocity distributions are not shown because they are not as extreme as the shroud and, in general, are not as difficult to control as the shroud velocity.) It can be seen that the velocity distribution varies considerably with the value of n . It appears that case D with $n = 2.0$ has the minimum peak velocity. Case F with $n = 2.5$ has a peak velocity not much higher than case D but a large region of nearly constant velocity. However, since case F has a significantly better radial profile than case D, it is considered the best of the four.



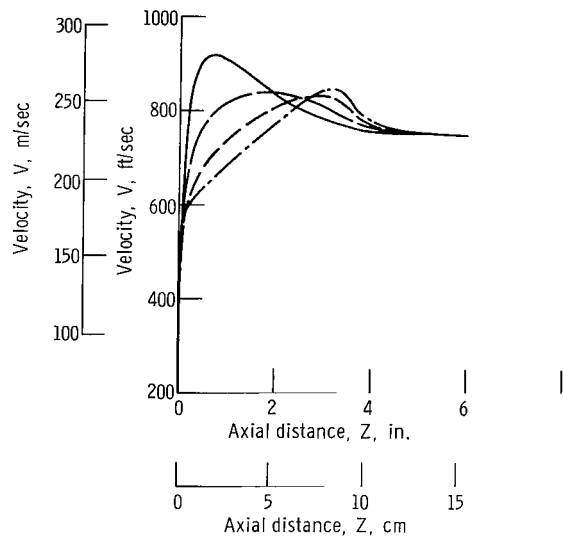
(a) Inlet geometry.



(b) Curvature distribution.



(c) Passage velocity profile. Control station depth, 3.5 inch (8.89 cm); control station depth to passage height ratio, 0.952.



(d) Shroud-surface-velocity distribution.

Figure 10. - Effect of superellipse exponent on potential-flow solution. Control-station velocity, V_c , 750 feet per second (229 m/sec).

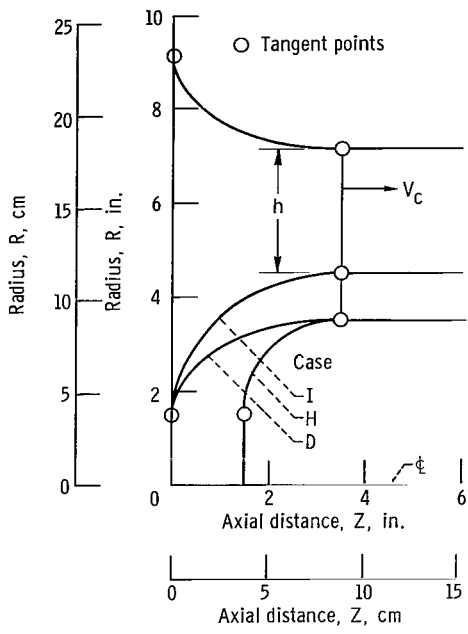
The optimum velocity distribution is one in which no local peak is reached so that there is no deceleration. However, this optimum does not appear to be attainable for the particular location of tangent points chosen for these cases, at least not by the use of the superellipse. A plot of peak velocity against n indicates the smallest peak velocity occurs around $n = 2.0$. This smallest peak is still greater than the average velocity at the control station. Based on these results, it appears that the optimum value of n lies between 2.0 and 2.5; however, an ordinary ellipse ($n = 2.0$) is certainly adequate. This conclusion should also apply to inlets having a bellmouth depth to passage height ratio close to 0.952, the value of the present cases.

Effect of Centerbody Variables

To determine the effect of the centerbody on the inlet velocity distribution, case D was modified in two different ways: the hub was shortened (case H), and the hub-tip ratio was increased (case I) as shown on figure 11(a). Case I is a different kind of variation from all the previous ones, in that the area of the downstream duct is reduced; however, for the potential flow solution, the same average downstream velocity was specified.

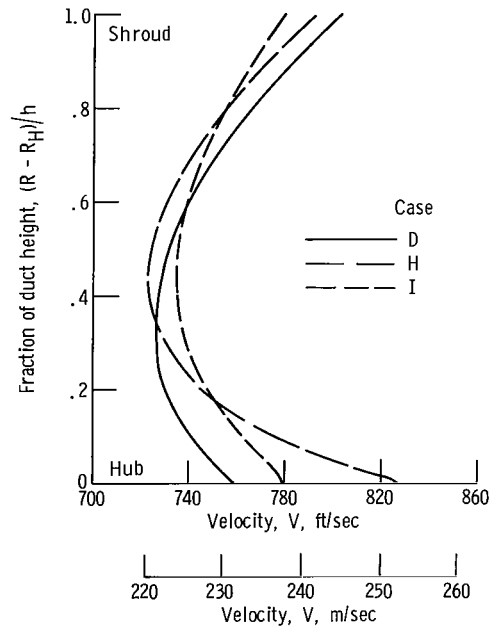
The passage velocity profiles for these configurations are shown on figure 11(b), and the shroud- and hub-velocity distributions are shown on figure 11(c). Since case I has a different duct height from cases D and H, the velocity profiles are plotted against fraction of duct height rather than radius in order to facilitate visual comparison. In both cases (H and I) the radial velocity gradient has steepened near the hub but has not changed appreciably near the shroud. And in both cases, the shroud-surface-velocity distribution has improved somewhat, but the hub-velocity distribution has peaked at higher velocities, with highest velocities obtained for case H. The steep radial gradient of case H at the hub is probably caused by the increased curvature resulting from the shortening of the hub while keeping the hub tangent point fixed at $Z = 3.5$ inches (8.89 cm). The change in the shroud-velocity distribution between cases D and I is probably the result of decreased passage height h making the local radius of curvature a greater percentage of the passage height, or, in other words, producing a smaller effective curvature.

Another comparison that illustrates the effect of shortening the hub is shown on figure 12. This is an inlet to a turbojet engine for which potential flow solutions were obtained with the centerbody nose located at $Z = 0$ (case TJ-1) and at $Z = 3.0$ inches (7.62 cm) (case TJ-2). The bellmouth is a circular arc. The long hub has a circular-arc nose (case TJ-1), and the short hub has an elliptical nose (case TJ-2) (fig. 12(a)). The passage velocity profiles at the compressor inlet station $Z = 6.0$ inches (15.24 cm)

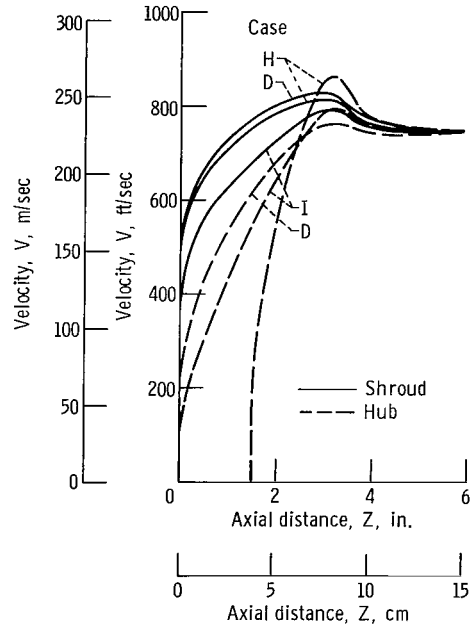


Case	Measuring station depth to passage height ratio, Z_M/h	Hub-tip ratio, R_H/R_S	Centerbody-nose depth to passage height ratio, Z_0/h
D	0.952	0.488	0
H	.952	.488	.408
I	1.308	.627	0

(a) Inlet geometry.

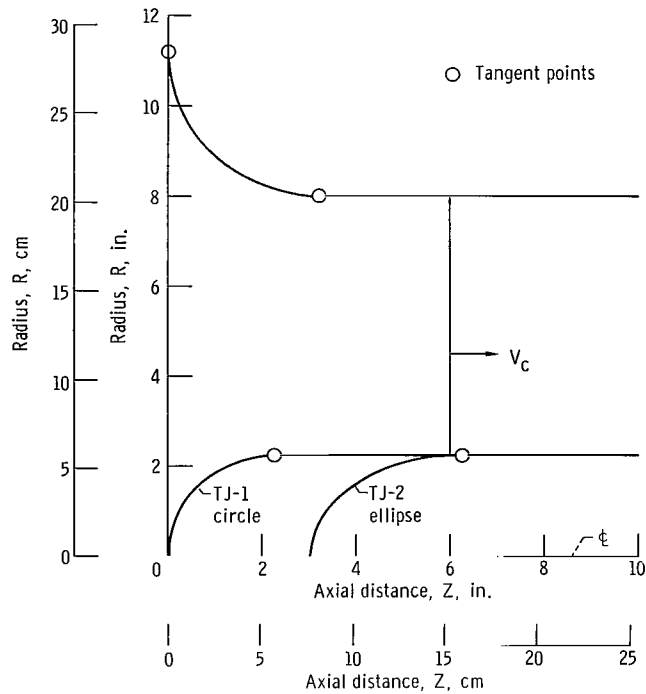


(b) Passage velocity profile. Measuring-station depth, 3.5 inches (8.89 cm).

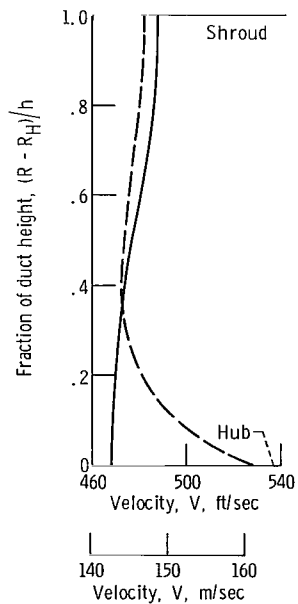


(c) Surface velocity distribution.

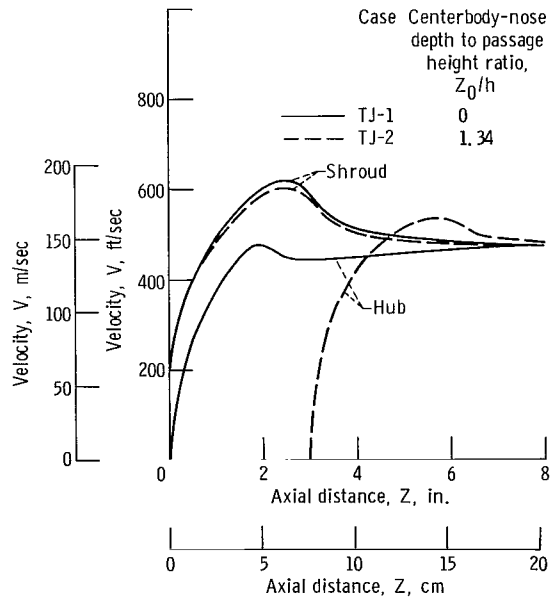
Figure 11. - Effect of centerbody variables on potential-flow solution. Control-station velocity, V_C , 750 feet per second (229 m/sec).



(a) Inlet geometry.



(b) Passage velocity profile. Axial distance, 6.0 inches (15.24 cm); measuring-station depth to passage height ratio, 1.042. Hub-tip



(c) Surface velocity distribution.

Figure 12. - Effect of centerbody location on potential-flow solution in turbojet inlet. Control-station velocity, 480 feet per second (140 m/sec); hub-tip ratio, 0.28.

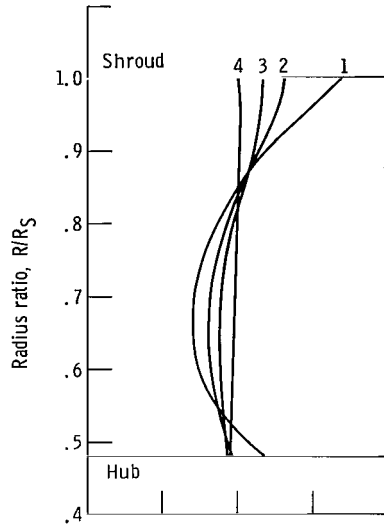
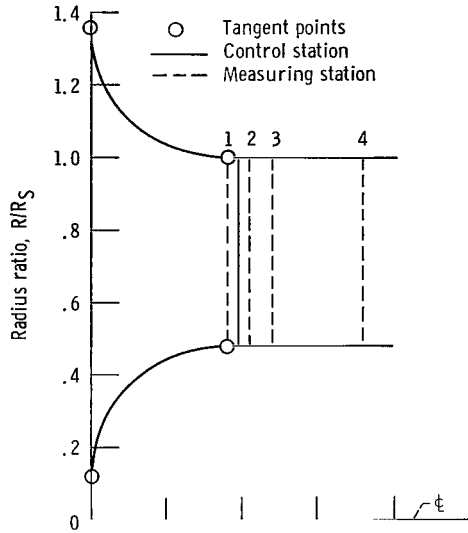
(fig. 12(b)) indicate that the significant influence of the hub change extends only about half-way across the channel. In figure 12(c), it can be seen that the change in the hub does not produce a very significant effect on the shroud-velocity distribution. Part of the reason for this lack of significant effect is the relatively low hub-tip ratio (0.28). The hub-velocity distributions are quite different because the nose shapes are different and because the shorter nose is almost entirely within the duct.

Based on these results, it appears that changes in centerbody variables have a significant effect on the flow only on or near the centerbody except in the case of relatively high hub-tip ratio.

Effect of Axial Depth on Passage-Velocity Profile

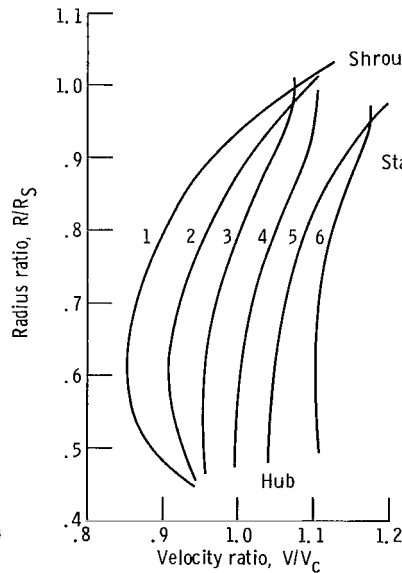
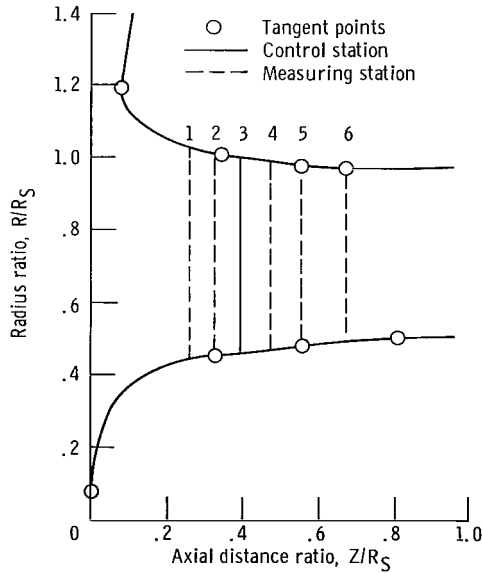
In a previous section the effect of a change in the depth or axial extent of the curved portion of an inlet on the velocity profiles across the passage at a fixed axial station was noted. In this section the velocity profiles at several axial stations will be given for two different inlets to illustrate the effect of axial depth in inlets of fixed curvature distribution. First, the inlet from reference 8 (previously discussed in the section Passage-Velocity Profile Data) will be considered. The geometrical configuration and the radial velocity profiles at several stations are shown on figure 13(a). The geometrical dimensions have been made dimensionless by dividing them by the control-station shroud radius, and the velocities have been made dimensionless by dividing the local velocity by the average velocity at the control station. The first station is in the plane of the tangent points so that all the stations are in the straight section. The radial velocity gradient is still significant at the $Z/R_S = 0.481$ station, which is 1/2 inch (1.27 cm) downstream of the tangent points because, even though the walls are straight, the passage streamlines still have curvature and slope. One inch (2.54 cm) further downstream at the $Z/R_S = 0.722$ station, the velocity is nearly constant.

Next, an inlet designed at the Lewis Research Center for a fan-in-wing installation is shown on figure 13(b). The geometric dimensions and the velocity have been non-dimensionalized in the same way as the inlet of figure 13(a). The configurations of figure 13 are nearly similar geometrically, but the figure 13(b) configuration is more complicated than the previous one in that both the hub and the shroud consist of first a curved section, then a sloping straight section, then another short curved section, and finally a downstream straight section. Passage velocity profiles at several stations are shown in the figure. All these stations are upstream of the final straight section, and, therefore, the velocity profiles do not straighten out as in figure 13(a). The most severe velocity variations are in the region of the upstream curved sections, that is, the bell-mouth. The variations begin to be damped out in the intermediate straight section, but



Station	Axial distance ratio, Z/R_S	Axial distance to passage height ratio, Z/h
1	0.361	0.694
2	.421	.809
3	.481	.924
4	.722	1.388

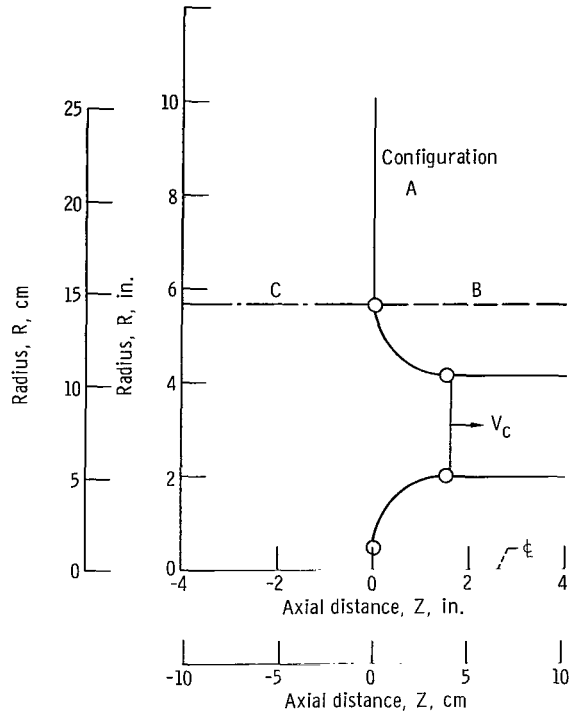
(a) Inlet configuration of reference 8.



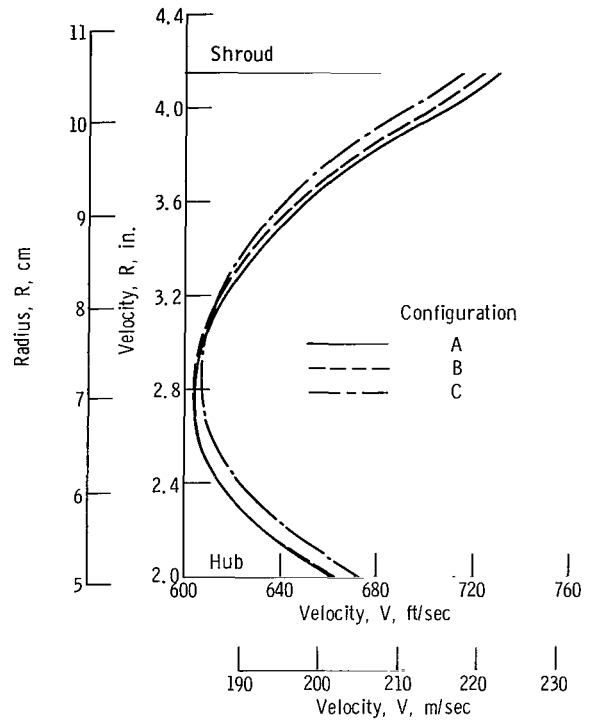
Station	Axial distance ratio, Z/R_S	Axial distance to passage height ratio, Z/h
1	0.265	0.492
2	.331	.616
3	.397	.739
4	.476	.887
5	.556	1.035
6	.675	1.256

(b) Inlet designed for fan-in-wing installation.

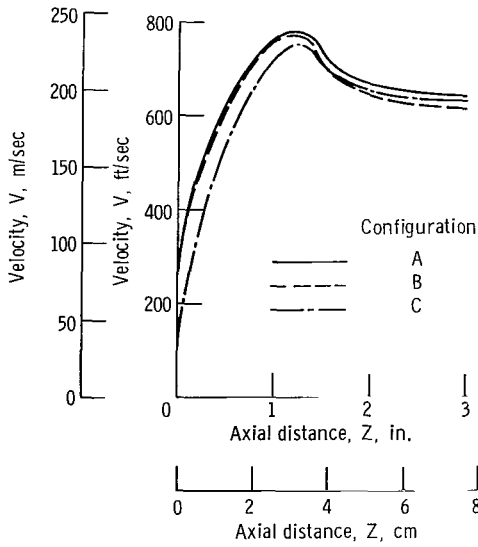
Figure 13. - Effect of axial depth on passage velocity profile.



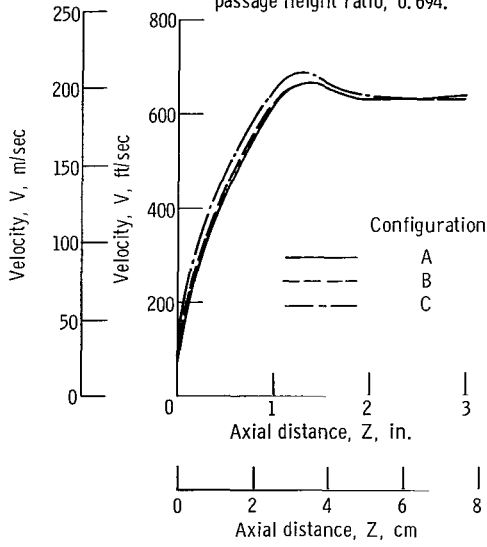
(a) Geometric configurations.



(b) Passage velocity profile. Axial depth, 1.5 inches (3.81 cm); axial depth to passage height ratio, 0.694.



(c) Shroud-surface-velocity distribution.



(d) Hub-surface-velocity distribution.

Figure 14. - Effect of inlet installation on potential-flow solution. Control-station velocity, V_c , 640 feet per second (195 m/sec).

increase again in the region of the downstream curved sections. In addition to the local wall curvature effects just mentioned, it is noted that the average velocity level increases with increasing axial distance because of the decreasing annular area and that the velocity is higher near the shroud than near the hub as a residual effect of the entrance flow pattern into the bellmouth.

Effect of Inlet Installation

As indicated in figure 1, there are other types of VTOL inlet installations of interest in addition to the fan-in-wing. To determine how the flow in a given inlet is affected by the particular installation, the inlet of figures 4 and 13(a) was analyzed for the range of installations shown in figure 1. Idealization of these installations can be established as shown in figure 14(a).

Configuration A is the idealization of a fan-in-wing inlet previously discussed in detail (fig. 2). Configuration B represents an inlet (for lift fan or engine) installed in a pod, platform, or fuselage (see figs. 1(c) and (d)). Configuration C represents an inlet (for a lift fan) installed in a platform adjacent to the fuselage (see fig. 1(b)). Configuration C is a rather extreme limiting case of the real installation in that the fuselage is represented by an axisymmetric duct attached to the inlet bellmouth (at the tangent point on figure 14(a)).

Potential flow solutions were obtained for the three configurations of figure 14(a) and results are shown for radial velocity profiles in figure 14(b), shroud surface velocities in figure 14(c), and hub surface velocities in figure 14(d). It can be seen that the results of configurations A and B are quite close, and those of configuration C are not greatly different. Furthermore, since the effect of the configuration C installation is felt almost as much on the hub as on the shroud, this is a duct effect rather than a local wall effect; thus, a more realistic representation of the platform inlet should yield an insignificant effect.

In general, based on these results, it appears that the potential flow in an inlet will not be significantly affected by differences in installation. Thus, the results for fan-in-wing inlets presented herein should be applicable to other types of VTOL inlet installations.

DESIGN APPLICATIONS

The ability of the potential flow solutions to predict the surface velocity distributions and the radial velocity profiles rather well makes it extremely useful in designing an in-

let for a lift fan or lift engine and also as an aid in the design of the fan itself. These applications will be discussed in relation to an actual fan-in-wing design.

Inlet Geometry

The potential flow solution described herein is an analysis method (one which produces velocities from a given geometry) rather than a design method (one which produces the geometry from given velocities). Thus, its use as a design tool consists of a trial and error scheme of screening particular prescribed configurations until a satisfactory one is attained. In general, a satisfactory inlet is one that has a minimum deceleration of velocity on the bellmouth and centerbody surfaces and a minimum radial variation in velocity at the rotor inlet in a minimum of axial depth. These are conflicting requirements and, therefore, must be compromised. Furthermore, there are not as yet available clear-cut quantitative measures or criteria for these requirements, and as a result, their relative merits must be evaluated in an intuitive way. The determination of an inlet section for a lift fan installed in a wing will now be discussed as an example of the application of the method.

The basic constraints of the problem fixed prior to the inlet design were a nominal fan rotor tip diameter of 15 inches (26.67 cm), a hub-tip ratio of about 0.45, and a 54-inch (137.2-cm) chord wing of profile NACA 65₃A (218)-217 with the fan centerline located at the 40-percent chord point. Other design conditions specified were a mass flow rate of about 40 pounds mass per second (18.144 kg/sec), which results in an average axial velocity at the rotor inlet of 650 feet per second (198 m/sec), and an area ratio across the rotor of 0.915. Initially, a straight section across the rotor tip was also specified.

The chordwise section of the wing and the inlet are shown in figure 15. For this wing profile, the upper wing surface is nearly symmetrical about the fan centerline; consequently, it was assumed that the fore and aft portions of the inlet have the same profile.

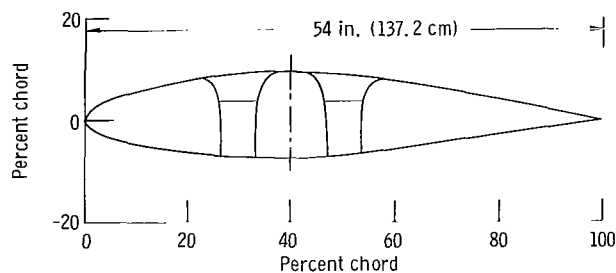


Figure 15. - Profile of NACA 65₃A(218)-217 airfoil showing fan inlet location.

Thus, only one profile has to be designed in the chordwise plane.

Design trials. - Four design trials (including the final design) will be discussed. The four configurations are shown on figure 16, parts (a) to (d). All configurations are constructed of superellipses and straight lines; the exponent n (eq. (13)) is shown in the figure (an exponent of 1.0 indicates a straight line). The velocity profiles across the passage at the rotor inlet stations of the several trials are shown on figure 16(e), and the shroud-surface-velocity distributions are shown on figure 16(f). Each trial will be discussed individually and reasons will be given for modifying it or, in the case of the final design, of accepting it.

An early profile is shown in figure 16(a) as trial A. The key dimensions here are a rotor inlet depth of 1.6 inches (4.06 cm) and the wing tangent point located at $Z = 0.8$ inch (2.03 cm) and $R = 10$ inches (25.4 cm). The rotor-tip straight section is tangent to the bellmouth at the rotor inlet at $Z = 1.6$ inches (4.06 cm) and $R = 7.5$ inches (19.05 cm). The velocity profile at the rotor inlet station is shown on figure 16(e) and the bellmouth surface-velocity distribution on figure 16(f). It can be seen that the deceleration on the shroud and the radial variation of velocity are both quite severe and were thus deemed unsatisfactory.

In an attempt to alleviate the severe deceleration on the shroud of case A, the straight section at the rotor tip was eliminated and the wing tangent point was moved in toward the axis. These changes produced a more trumpet-like inlet (trial B of fig. 16(b)). The surface-velocity distribution is shown in figure 16(f) and the radial velocity profile in figure 16(e). The bellmouth surface-velocity distribution has improved significantly over trial A; however, the velocity profile has hardly changed at all.

Even though the surface-velocity distribution of trial B may have been adequate, in order to improve the passage-velocity profile, the depth of the rotor inlet was increased to 2.0 inches (5.08 cm). In addition, it was decided, primarily for mechanical reasons, to go back to the straight section across the rotor tip. Trial C is one of the attempts made with these conditions as shown on figure 16(c). The velocity profile is shown on figure 16(e), and the surface velocity on figure 16(f). The velocity profile has improved over trials A and B; however, the surface velocity has regressed to being almost as poor as trial A. Trial C was therefore also judged to be unacceptable.

After the experience of the three trials shown and others, it was decided to relax somewhat the requirement of a very shallow bellmouth and move the rotor inlet to a depth of 3.0 inches (7.62 cm). At the same time, it was decided to make the hub contour at the rotor root a straight line and to change the values of tip and hub radius slightly. After a few trials a final design, trial D, was attained as shown on figure 16(d). The velocity profile across the passage is shown on figure 16(e), and the hub and shroud velocity distributions are shown on figure 16(f). Although the hub plays a minor role in the design procedure the final hub-velocity distribution is also shown for com-

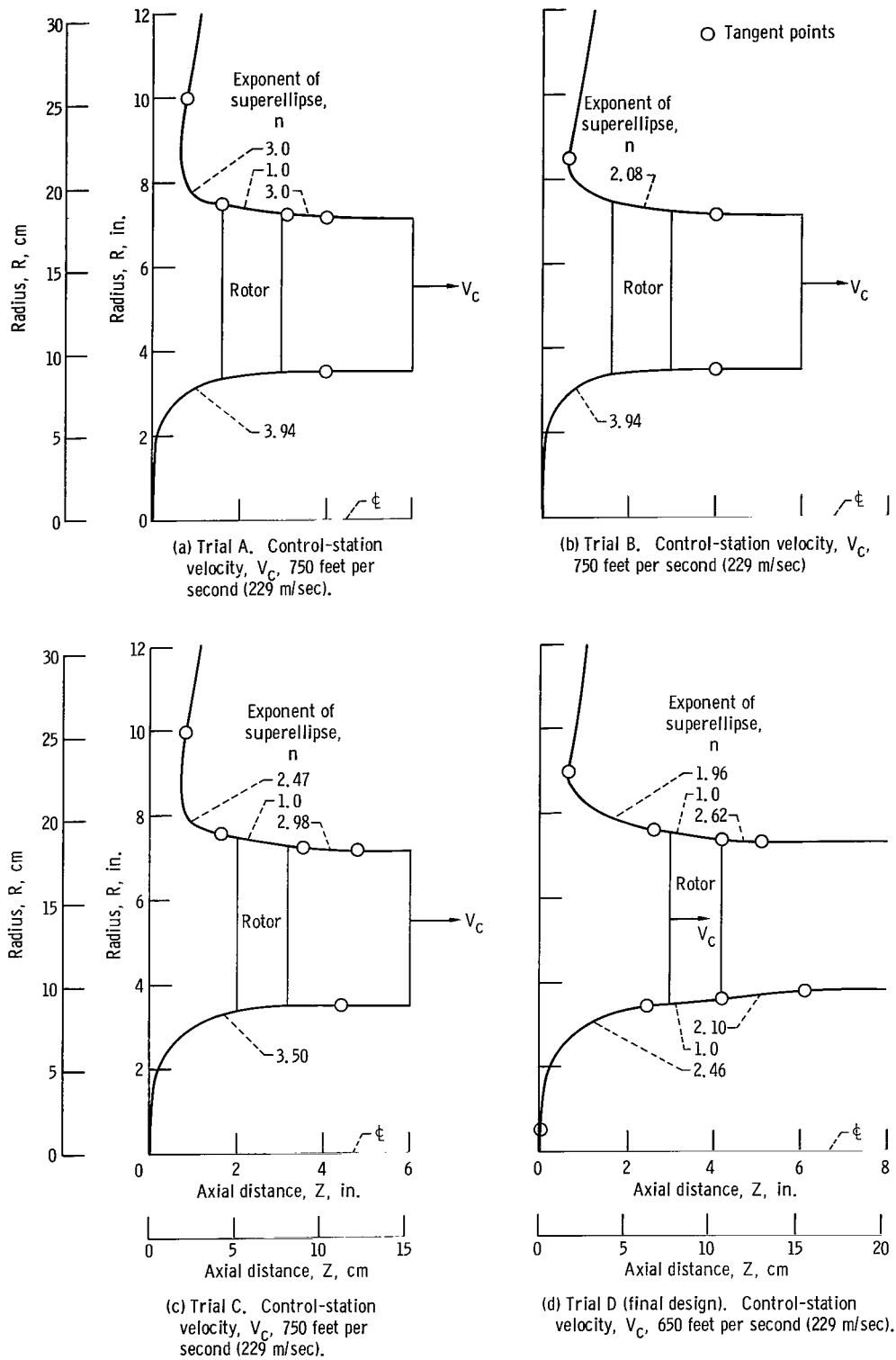


Figure 16. - Fan-inlet design trials.

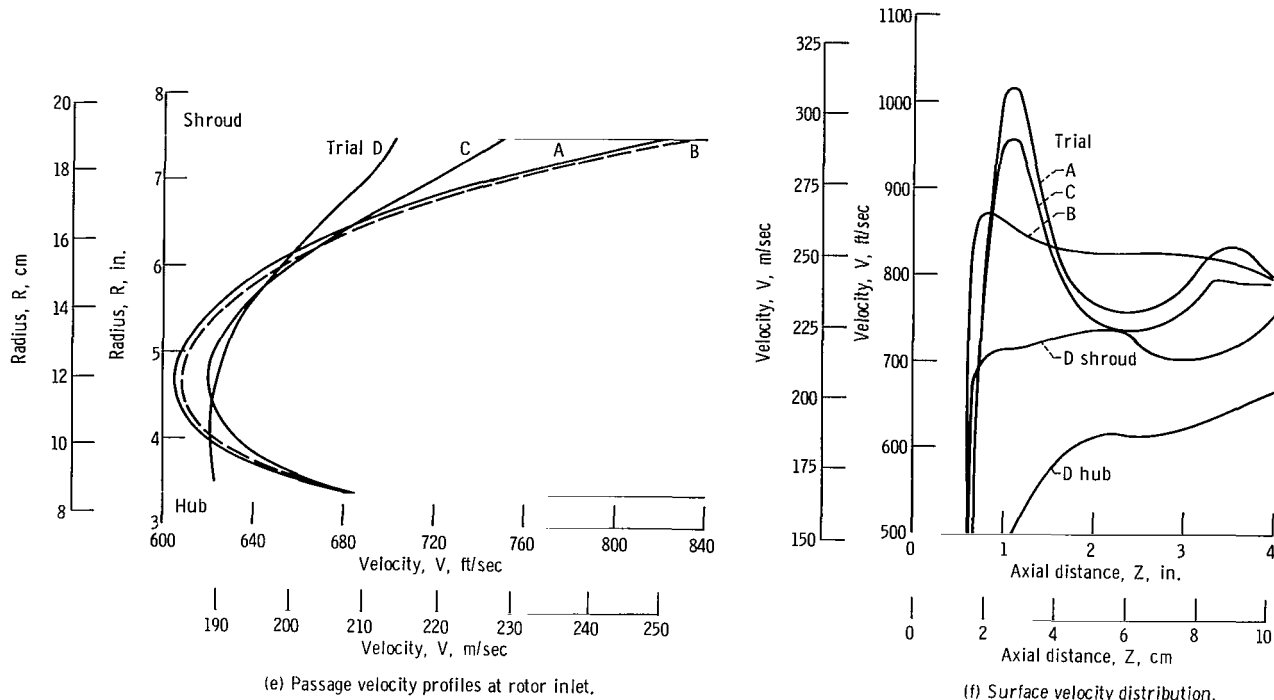


Figure 16. - Concluded.

pleteness. The straight rotor root accounts for the straightening out of the velocity profile near the hub.

Comparison of the several trials in figures 16(e) and (f) indicates that both the surface-velocity distribution and the passage profile of the final design are better than any of the previous trials. Although they could probably be improved further, they were considered acceptable, and it was evident that the point of diminishing returns had been reached in the trial and error scheme.

Axial asymmetry. - The velocities just presented for the final design are actually those for an axially symmetric inlet having the contour shown previously in figure 16(d). The actual fan-in-wing inlet is not axisymmetric; however, as was indicated previously, this asymmetry can be taken into account by analyzing the profile of other meridional planes at various angles to the chordwise plane. In the case under consideration, these other profiles must still be designed. The primary considerations are that these other profiles must fit well with the final chordwise profile in the region of asymmetry near the wing surface and must coincide with the chordwise profile from some point ahead of the rotor to produce an axisymmetric passage. If these conditions are not met, the rotor may encounter unnecessary circumferential distortion.

For the spanwise profile, the problem is similar to that of designing the chordwise profile, except that there is not as much freedom because the spanwise profile must

coincide with the chordwise profile downstream of some point ahead of the rotor. After a few trials, this point was fixed at $Z = 0.987$ inch (2.5 cm) and $R = 8.306$ inches (21.1 cm). The only remaining point to be chosen is the tangent point to the wing, and this was finally fixed at $R = 11.0$ inches (27.94 cm). The final profile (a superellipse satisfying the constraints given) is shown in figure 17(a) as the 90° profile. The 0° profile is the same as in figure 16(d).

Additional meridional profiles at several other circumferential locations must also be determined. In this particular inlet, only one quadrant of meridional profiles need be designed to determine the full annular passage since fore and aft symmetry was assumed; that is, the profile at, say 15° , recurs at -15° , 165° , and -165° . In designing the intermediate profiles, only one point, the tangent point to the wing is undetermined because the point of incipient axial symmetry has been fixed in the design of the spanwise or 90° profile. The wing tangent points were determined for all circumferential locations by requiring that they lie on a straight line connecting the tangent points of the chordwise and spanwise profiles. The resulting 45° profile is shown in figure 17(a). For such a configuration, it may be necessary to generate profiles every 15° to adequately specify the resulting three-dimensional shape.

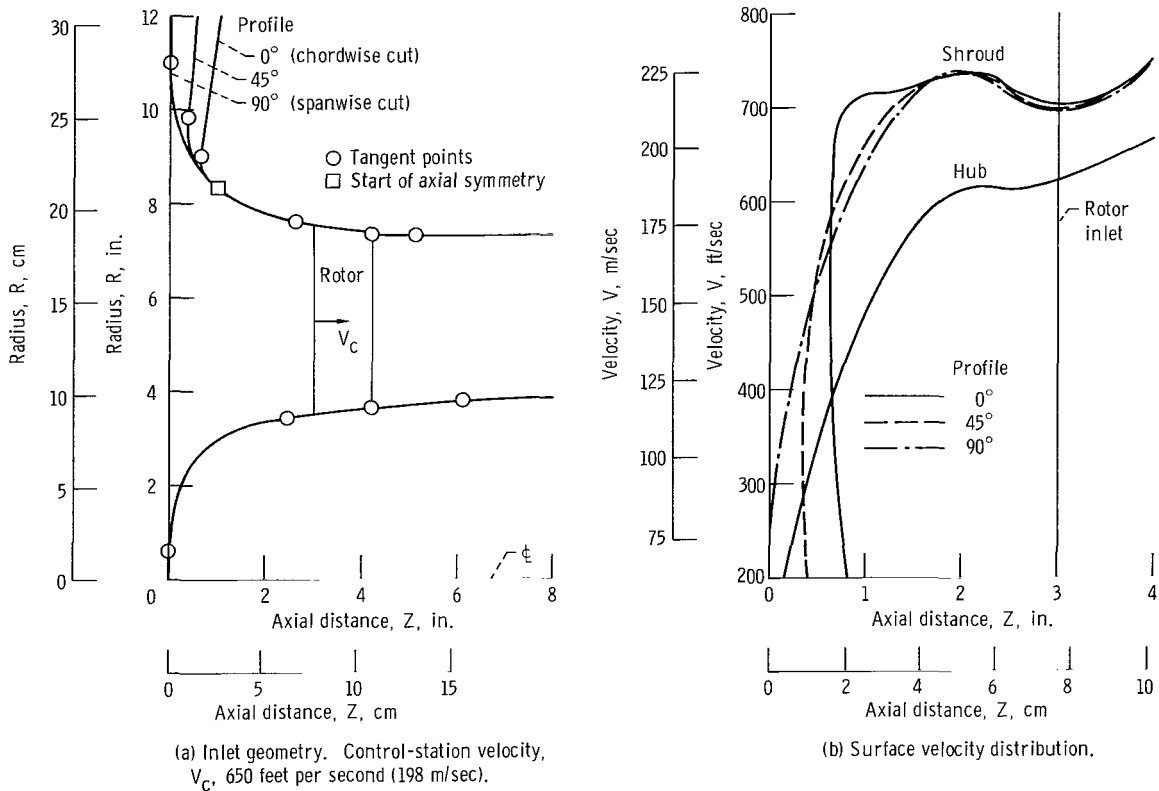


Figure 17. - Fan-inlet final design showing axial asymmetry.

Potential flow solutions were obtained at several of the circumferential stations to complete the inlet velocity pictures. The hub and shroud surface velocity distributions for the 0° , 45° , and 90° profiles are shown on figure 17(b). The hub velocity is essentially the same for all three profiles so only one curve is shown. The passage velocity profiles are not shown because they do not differ significantly from the 0° case (trial D of fig. 16(e)). It can be seen that the difference in velocity caused by the asymmetry extends somewhat into the axisymmetric region ($Z > 0.987$ in. or 25 cm) but that a significant difference does not extend into the region of interest near the rotor inlet ($Z = 3.0$ in. or 7.62 cm).

Rotor Considerations

The calculation of the flow in the inlet section can provide several useful inputs required for the design of the fan rotor. Blade-design calculations, based on methods that include streamline curvature through the blade rows, require input values of streamline location and slope as well as velocity components at the inlet to the first blade row of the stage (rotor). Such values can be supplied directly by the inlet flow solution. However, it should be recognized that the physical presence of a blade row will necessarily alter the streamline flow as determined for the inlet section alone in the immediate vicinity of the leading edge of the rotor. This distortion of the potential-flow streamlines arises from the effects of radial variations of blade thickness (e.g., ref. 17) and blade-pressure ratio and of the growth of the casing boundary layers across the blade row.

The magnitude of the resultant distortion of the streamlines at the rotor inlet will depend on the magnitude of the net radial displacement of the streamlines across the rotor blade row and on the aspect ratio of the blade row. Thus, a truly accurate solution of the rotor blade-row inlet flow will require a coupling of the inlet-section solutions and the blade-row velocity-diagram solutions, or a complete three-dimensional (blade-to-blade) solution. However, in the absence of such procedures, the inlet-section potential flow solution can be used as a first approximation for the required inputs. There are two preliminary approaches that might be used in this respect.

In the first approach, the reference inlet streamlines for the rotor design calculation are first taken from the potential-flow solution at the leading edge of the rotor blade row. An initial calculation is then made of fan blade-row outlet flows. A fairing can then be made between the various fan blade-row streamline positions and the streamlines in the inlet section (from the potential flow solution) some distance upstream of the rotor leading edge where the blade-row effects are judged to be no longer significant (say, order of $1/2$ to 1 axial chord length). This fairing would require some judgment or insight in order to approximate the effects of the blade-row thickness distribution and wall boundary-

layer development. This procedure, depending on proper convergence, can then provide a modified flow variation at the rotor leading edge, which can then be used for the design of the rotor blade profile sections.

In the second approach, the upstream conditions for the rotor calculation are taken from the potential flow solution at the undisturbed upstream station. The rotor blade-row calculation program, by iteration, then establishes a revised flow distribution at the rotor leading-edge station. In this procedure, the inlet streamlines are adjusted for effects of streamline displacement at the rotor outlet. Some further modifications will have to be made to include the effects of blade thickness and wall boundary-layer variations, if desired.

The inlet section flow solution can also supply bellmouth velocity distributions for the estimation of the entrance boundary layer at the tip of the rotor. The characteristics of the entrance boundary layer are known to influence rotor performance, and such data may provide some insight into the possible effects on tip-region efficiency and range of operation. The inlet section solution method can also provide an indication of the maximum circumferential distortion of static pressure and velocity at the inlet to a rotor for the case of an asymmetric inlet. These values can be obtained from a number of successive axisymmetric solutions covering the varying profiles of the inlet section.

CONCLUDING REMARKS

The usefulness of an incompressible axisymmetric potential flow solution as a tool in the analysis and design of VTOL inlets in static operation has been illustrated. The analysis adequately predicts results for compressible flow (providing there is no boundary-layer separation). A plane two-dimensional potential flow solution adequately predicts results for axisymmetric inlets on the shroud but not on or near the hub. For the range of inlet geometry variables covered, a trumpet shaped inlet is best for minimizing surface velocity gradients, while increased depth is best for reducing radial velocity variations. The hub-surface-velocity gradients are small compared with the shroud-surface-velocity gradients. It was also found that the flow distributions in the inlet section are negligibly affected by the type of installation, that is, wing, pod, or platform.

Lewis Research Center,
National Aeronautics and Space Administration,
Cleveland, Ohio, October 28, 1968,
721-03-00-24-22.

APPENDIX - SYMBOLS

<p>a major axis of superellipse, eq. (5)</p> <p>a_t stagnation speed of sound</p> <p>b minor axis of superellipse, eq. (5)</p> <p>h annular passage height at control station, $R_S - R_H$</p> <p>K curvature</p> <p>n distance along \bar{n} and exponent of superellipse, eq. (5)</p> <p>\bar{n} unit vector normal to surface</p> <p>P pressure</p> <p>ΔP_S difference between local static pressure and ambient pressure, $P_S - P_t$</p> <p>q dynamic pressure</p> <p>R radius coordinate or gas constant</p> <p>r radius of curvature</p> <p>S surface distance</p> <p>T temperature</p> <p>V velocity</p> <p>\bar{V} velocity vector</p>	<p>x rectangular coordinate in superellipse equation</p> <p>y rectangular coordinate in superellipse equation</p> <p>Z axial distance</p> <p>δ distance between bellmouth tangent point and measuring station (fig. 4)</p> <p>ρ density</p> <p>Φ velocity potential</p> <p>Subscripts:</p> <p>a bulk conditions of inlet channel flow at control station</p> <p>av average</p> <p>c control station</p> <p>H hub</p> <p>M measuring station</p> <p>R component in R direction</p> <p>S shroud</p> <p>s static</p> <p>t total</p> <p>Z component in Z direction</p> <p>0 centerbody nose</p>
--	---

REFERENCES

1. Campbell, John Paul: Vertical Takeoff and Landing Aircraft. The Macmillan Co., 1962.
2. Schaub, U. W.; and Cockshutt, E. P.: Analytic and Experimental Studies of Normal Inlets, with Special Reference to Fan-in-Wing VTOL Powerplants. Proceedings of the 4th International Council of the Aeronautical Sciences Congress. R. R. Dexter, ed., Spartan Books, Inc., 1965, pp. 519-553.
3. Schaub, U. W.; Bassett, R. W.; and Cockshutt, E. P.: An Investigation of the Aerodynamics of Intakes in the Upper Surface of a Wing. Canada, Nat. Res. Council, Div. Mech. Eng. and Nat. Aeron. Establ. Quarterly Bull. no. 4, 1966, pp. 69-99.
4. Barche, Jürgen: Beitrag zur Gestaltung von Einläufen für Hubtriebwerke. Zeit. für Flug. vol. 15, no. 3, Mar. 1967, pp. 98-109.
5. Smith, A. M. O.: Incompressible Flow about Bodies of Arbitrary Shape. Paper No. 62-143, Inst. Aerospace Sci., June 1962.
6. Schaub, U. W.: Fan-in-Wing Aerodynamics - Experimental Assessment of Several Inlet Geometries. Paper No. 67-746, AIAA, Oct. 1967.
7. Schaub, U. W.: Experimental Investigation of Flow Distortion in Fan-in-Wing Inlets. J. Aircraft, vol. 5, no. 5, Sept.-Oct. 1968, pp. 473-478.
8. Schaub, U. W.; and Bassett, R. W.: Analysis of the Performance of a Highly Loaded 12-Inch VTOL Z-Axis, Fan-in-Wing Model at Zero Forward Speed. Rep. LR-439, National Research Council of Canada, Sept. 1965.
9. Fowler, H. S.: Some Tests of 12-In. Dia. Model VTOL Ducted Fans. Rep. LR-367, National Research Council of Canada, 1962.
10. Gregory, N.; Raymer, W. G.; and Love, Edna M.: The Effect of Forward Speed on the Inlet Flow Distribution and Performance of a Lifting Fan Installed in a Wing. Rep. ARC R&M-3388, Aeronautical Research Council, Great Britain, 1965.
11. Rubbert, P. E.; and Saaris, G. R.: A General Three-Dimensional Potential-Flow Method Applied to V/STOL Aerodynamics. Paper No. 680304, SAE, Apr. 1968.
12. Smith, A. M. O.; and Pierce, Jesse: Exact Solution of the Neumann Problem. Calculation of Non-Circulatory Plane and Axially Symmetric Flows about or within Arbitrary Boundaries. Rep. ES-26988, Douglas Aircraft Co., Inc., Apr. 25, 1958.

13. Hess, J. L.; and Smith, A. M. O.: Calculation of Potential Flow about Arbitrary Bodies. Progress in Aeronautical Sciences. Vol. 8. D. Kuchemann, ed., Pergamon Press, 1967, pp. 1-138.
14. Hess, John L.; and Smith, A. M. O.: A General Method for Calculating Low Speed Flow about Inlets. Aerodynamics of Power Plant Installation, part 1. AGARDograph 103, pt. 1, 1965, pp. 345-372.
15. Chironis, Nicholas P.: Between Circle and Square Lie the Handy Super-Curves. Product Eng., vol. 38, no. 9, Apr. 24, 1967, pp. 52-55.
16. Przedpelski, Zygmunt J.: Lift Fan Technology Studies. NASA CR-761, 1967.
17. Stanitz, John D.: Effect of Blade-Thickness Taper on Axial-Velocity Distribution at the Leading Edge of an Entrance Rotor-Blade Row with Axial Inlet, and the Influence of this Distribution on Alinement of the Rotor Blade for Zero Angle of Attack. NACA TN 2986, 1953.

FIRST CLASS MAIL

05U 001 26 51 30S 69033 00903
AIR FORCE WEAPONS LABORATORY/AFWL/
KIRTLAND AIR FORCE BASE, NEW MEXICO 87117

ATTN: DR. R. L. YALOW, ACTING CHIEF TECH. LIAISON

POSTMASTER: If Undeliverable (Section 158
Postal Manual) Do Not Return

"The aeronautical and space activities of the United States shall be conducted so as to contribute . . . to the expansion of human knowledge of phenomena in the atmosphere and space. The Administration shall provide for the widest practicable and appropriate dissemination of information concerning its activities and the results thereof."

— NATIONAL AERONAUTICS AND SPACE ACT OF 1958

NASA SCIENTIFIC AND TECHNICAL PUBLICATIONS

TECHNICAL REPORTS: Scientific and technical information considered important, complete, and a lasting contribution to existing knowledge.

TECHNICAL NOTES: Information less broad in scope but nevertheless of importance as a contribution to existing knowledge.

TECHNICAL MEMORANDUMS: Information receiving limited distribution because of preliminary data, security classification, or other reasons.

CONTRACTOR REPORTS: Scientific and technical information generated under a NASA contract or grant and considered an important contribution to existing knowledge.

TECHNICAL TRANSLATIONS: Information published in a foreign language considered to merit NASA distribution in English.

SPECIAL PUBLICATIONS: Information derived from or of value to NASA activities. Publications include conference proceedings, monographs, data compilations, handbooks, sourcebooks, and special bibliographies.

TECHNOLOGY UTILIZATION PUBLICATIONS: Information on technology used by NASA that may be of particular interest in commercial and other non-aerospace applications. Publications include Tech Briefs, Technology Utilization Reports and Notes, and Technology Surveys.

Details on the availability of these publications may be obtained from:

SCIENTIFIC AND TECHNICAL INFORMATION DIVISION
NATIONAL AERONAUTICS AND SPACE ADMINISTRATION
Washington, D.C. 20546